A Growth Model of Gas Hydrates in Water-in-Oil Emulsion Flow

Carlos Lange-Bassani, Jean-Michel Herri, Amadeu K. Sum, Rigoberto E.M. Morales, Ana Cameirão

HAL Id: emse-02562337

https://hal-emse.ccsd.cnrs.fr/emse-02562337v1

Submitted on 4 May 2020

A Growth Model of Gas Hydrates in Water-in-Oil Emulsion Flow

C.L. Bassani[1,2], J.M. Herri[1], A.K. Sum[3], R.E.M. Morales[2*] and <u>A. Cameirão</u>[1*]

[1]Mines Saint-Etienne, Univ Lyon, CNRS, UMR 5307 LGF, Centre SPIN, Departement PEG, F - 42023 Saint-Etienne France
[2]Multiphase Flow Research Center (NUEM), Federal University of Technology – Paraná (UTFPR), Rua Deputado Heitor Alencar Furtado, 5000, Bloco N, CEP 81280-340, Curitiba/PR, Brazil
[3]Hydrates Energy Innovation Laboratory, Chemical and Biological Engineering Department, Colorado School of Mines, 1500 Illinois St., Golden, CO 80401, USA

*rmorales@utfpr.edu.br; cameirao@emse.fr

Abstract. The correct prediction of gas hydrate formation is important to estimate pipeline blockage (plugging) in oil and gas production operations. This study presents a revisited model for growth of gas hydrates in water-in-oil emulsion flow. Literature points out that hydrates form as shells around the water droplets. The water core shrinkage rate (inward growth) is related to gas diffusion through the hydrate shell, while water permeation through the hydrate shell is the limiting phenomenon for outward growth. The models of literature are herein corrected (consideration of gas solubility in the hydrate shell, consideration of gas concentration along the shell coupled with gas consumption in the outer surface, coupling between gas absorption by the bulk and gas consumption due to hydrate formation) and extended for considering the crystal integration process in the outer particle surface and the mass transfer between the particle and the bulk. The model is compared to experimental data and the trend of the gas consumption over time due to hydrate formation is validated.

Introduction

The high pressure and low temperature conditions commonly found in offshore oil & gas production scenarios favor the formation of gas hydrates. Gas hydrates are crystals formed by the imprisonment of gas molecules (e.g., light hydrocarbons) in cages formed of hydrogen-bonded water molecules [1]. This crystal grows and agglomerates as it flows along the pipeline, causing eventual blocks with related production stop and revenue losses.

Gas hydrates form as shells contouring water droplets in the case of water-in-oil emulsion flow [2]. This hydrate shell is related to gas diffusion and water permeation resistances for the crystal growth kinetics [3,4]. The hydrate formation rate, by its turn, is related to the gas consumption rate along the pipeline, which cause flow deceleration [5], promoting settling of the slurry [6] once the deposition critical velocity is reached [7]. Several growth kinetic models have been proposed in literature to estimate the gas hydrate formation rate (see Ribeiro Jr and Lage [8] and Yin et al. [9] for a compilation of kinetic models), but predictive models for gas-oil-water systems are yet scarce [3,4].

The present study extends the models of Turner et al. [3] and Shi et al. [4] considering: (i) the gas solubility in the hydrate shell; (ii) the crystal integration in the outer surface of the particle; (iii) the competition between gas absorption from the free gas phase by the bulk and the gas depletion due to hydrate formation as proposed in [10,11]; and (iv) the mass transfer between the particle and the bulk [11].

Mathematical model

Water is considered flowing as an emulsion, i.e., small and spherical droplets homogeneously distributed in oil continuous phase [12]. In this kind of system and whenever pressure and temperature conditions are favorable, gas hydrates form as a shell around the water droplets [2], as depicted in Fig. 1(a). The main phenomena associated to growth kinetics of this kind of particle is presented in Fig. 1(b-g). Gas is absorbed by the bulk while it depletes in gas as hydrates form (b). Inner growth is related to gas diffusion through the hydrate shell (d), which also competes with mass transfer between the particle and the bulk (c) and crystal integration process in the inner surface (e). The core shrinkage makes water from the core to be expulsed through the hydrate porous shell (f), thus turning possible crystal integration in the outer surface to happen (g), with consequent outer growth.
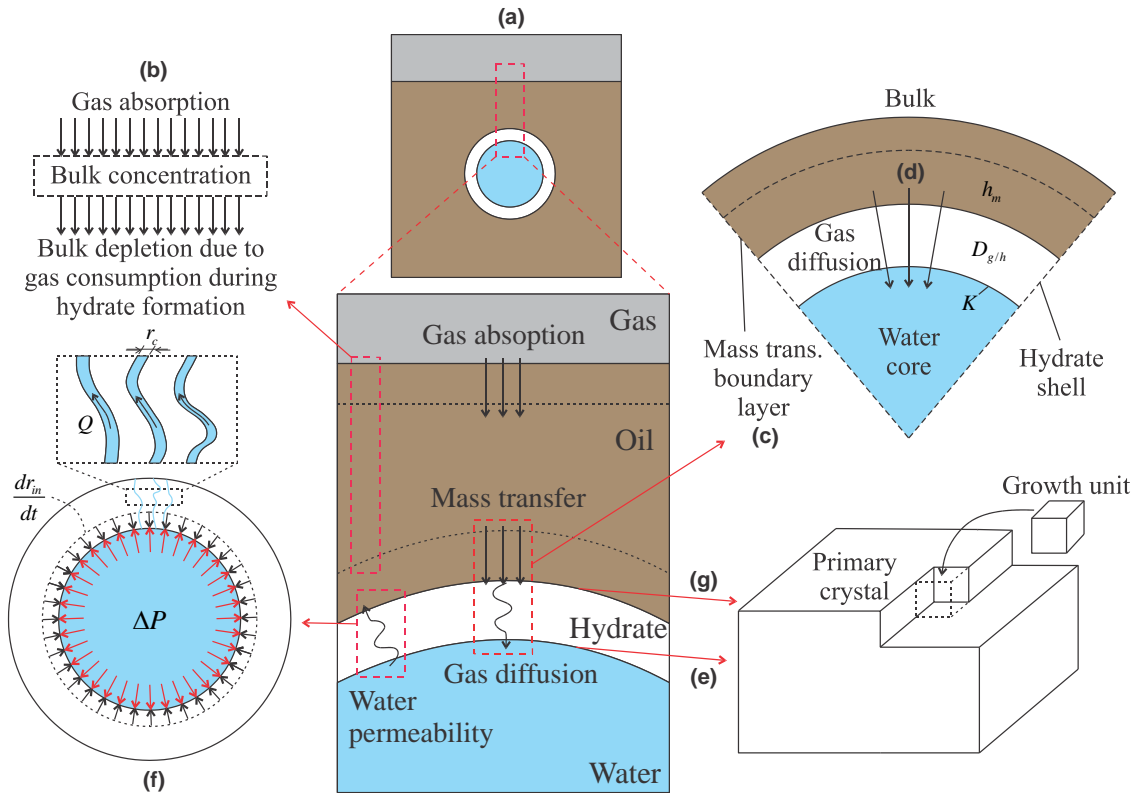

Figure 1. Depiction of mass transfer resistances in the growth kinetics of gas hydrate particles formed as shells contouring water droplets in oil continuous flow.

The gas concentration along the hydrate shell is calculated by Fick's Law in spherical coordinates, Eq. (1) (nomenclature section at the end of the article). The boundary conditions are the crystal integration in the inner surface of the particle and the mass transfer between the particle and the bulk in the outer surface, Eq. (2). The ODE solution is shown in Eq. (3).

$$\frac{d}{dr}\left(r^2 \frac{dC_h}{dr}\right) = 0 \tag{1}$$

$$-D_h A_{in,i} \frac{dC_h}{dr}\bigg|_{r=r_{in}} = -k_i A_{in,i}\left(\frac{C_h|_{r=r_{in}}}{H_w} - f_{eq}\right) \; ; \; -D_h A_{out,i} \frac{dC_h}{dr}\bigg|_{r=r_{out}} = h_m A_{out,i}\left(\frac{C_h|_{r=r_{out}}}{S_h} - C_b\right) - \frac{dn_{g,i}}{dt}\bigg|_{out} \tag{2}$$

$$C_h = C_{eq} + \frac{\left[\dfrac{1}{r_{in}} - \dfrac{1}{r} + \dfrac{1}{r_{in}^2}\dfrac{H_w D_h}{k_i}\right]}{\left[\dfrac{1}{r_{in}} - \dfrac{1}{r_{out}} + \dfrac{1}{r_{out}^2}\dfrac{S_h D_h}{h_m} + \dfrac{1}{r_{in}^2}\dfrac{H_w D_h}{k_i}\right]}\left[(S_h C_b - C_{eq}) - \frac{S_h}{h_m}\frac{1}{4\pi r_{out}^2}\left(-\frac{dn_{g,i}}{dt}\bigg|_{out}\right)\right] \text{ with } C_{eq} = H_w f_{eq} \tag{3}$$

The gas molar flux through the hydrate shell equals the amount of gas consumed to form hydrates in the inner growth and comes from derivation of Eq. (3), as shown in Eq. (4) (left). Yet knowing that hydrate formation follows the (pseudo)-stoichiometry of $1G + \eta H_2O \rightarrow (1+\eta)Hyd$, where η is the hydration number, then the hydrate formation is related to the gas consumption rate, Eq. (4) (right). Therefore, the linear growth rate of the inner surface of the particle $-dr_{in}/dt$ is related to the molar hydrate formation rate as shown in Eq. (5).

$$\left.\frac{dn_{g,i}}{dt}\right|_{in} = 4\pi r_{in}^2 D_h \left.\frac{dC_h}{dr}\right|_{r=r_{in}} \;\; ; \;\; \left.\frac{dn_h}{dt}\right|_{in} = (\eta+1)\left(-\left.\frac{dn_g}{dt}\right|_{in}\right) \tag{4}$$

$$\left.\frac{dn_{h,i}}{dt}\right|_{in} = -\frac{\rho_h}{M_h}\frac{d}{dt}\left(\frac{4}{3}\pi r_{in}^3\right) \;\rightarrow\; -\frac{dr_{in}}{dt} = (\eta+1)\frac{M_h}{\rho_h}\frac{(S_hC_b - C_{eq}) - \dfrac{S_h}{h_m}\dfrac{1}{4\pi r_{out}^2}\left(-\left.\dfrac{dn_{g,i}}{dt}\right|_{out}\right)}{\left[\dfrac{r_{in}^2}{D_h}\left(\dfrac{1}{r_{in}} - \dfrac{1}{r_{out}}\right) + \dfrac{H_w}{k_i} + \dfrac{S_h}{h_m}\dfrac{r_{in}^2}{r_{out}^2}\right]} \tag{5}$$

Outward growth is limited to water availability in the outer surface. Considering a fully rigid shell with no head loss in the capillaries, the water volumetric flowrate through the hydrate shell is the difference between the core volume shrinkage and the amount of water consumed to form hydrates, which are related to the inner growth rate as shown in Eq. (6). At maximum, all the permeated water will convert into hydrates instantly in the particle outer surface; but if enough water arrives at the particle outer surface, then crystal integration process may limit outer growth, Eq. (7). The linear outer growth rate is expressed in Eq. (8).

$$Q = \left(-\frac{d\forall_{core}}{dt}\right) - \left(-\left.\frac{d\forall_w}{dt}\right|_{in}\right) \;\rightarrow\; Q = 4\pi r_{in}^2\left[1 - \frac{\eta}{(\eta+1)}\frac{M_w}{M_h}\frac{\rho_h}{\rho_w}\right]\left(-\frac{dr_{in}}{dt}\right) \tag{6}$$

$$-\left.\frac{dn_{g,i}}{dt}\right|_{out} = \min\left[\frac{\rho_w}{\eta M_w}Q \; ; \; 4\pi r_{out}^2 k_i\left(\frac{C_{out,o}}{H_w} - f_{eq}\right)\right] \text{ with } C_{out,o} = \frac{C_h|_{r=r_{out}}}{S_h} \tag{7}$$

$$\frac{dr_{out}}{dt} = \frac{(\eta+1)}{4\pi r_{out}^2}\frac{M_h}{\rho_h}\min\left[\frac{\rho_w}{\eta M_w}Q \; ; \; 4\pi r_{out}^2\frac{k_i}{H_w}k_{out}\left(C_b - \frac{C_{eq}}{S_h}\right)\right] \text{ with } k_{out} = \left[1 - \frac{1}{h_m}\frac{k_i}{H_w} + \frac{\dfrac{S_h}{h_m}\dfrac{r_{in}^2}{r_{out}^2}}{\dfrac{r_{in}^2}{D_h}\left(\dfrac{1}{r_{in}} - \dfrac{1}{r_{out}}\right) + \dfrac{H_w}{k_i}}\right]^{-1} \tag{8}$$

The hydrate formation rate of the entire particle population is estimated by Eq. (9). The gas concentration in the bulk comes from a mass balance between the gas absorbed by the bulk and the gas consumed due to hydrate formation [10,11], Eq. (10).

$$\frac{dn_h}{dt} = \sum_i\left(\left.\frac{dn_{h,i}}{dt}\right|_{in} + \left.\frac{dn_{h,i}}{dt}\right|_{out}\right) = 4\pi\frac{\rho_h}{M_h}\sum_i\left(r_{out,i}^2\frac{dr_{out,i}}{dt} - r_{in,i}^2\frac{dr_{in,i}}{dt}\right) \tag{9}$$

$$\frac{dC_b}{dt} = \frac{k_{g/o}A_{g/o}}{\forall_o}\left(C_{g/o} - C_b\right) - \frac{1}{\forall_o}\frac{4\pi}{(\eta+1)}\frac{\rho_h}{M_h}\sum_i\left(r_{out,i}^2\frac{dr_{out,i}}{dt} - r_{in,i}^2\frac{dr_{in,i}}{dt}\right) \tag{10}$$

The model is composed of three ODEs for the inner growth rate (Eq. (5)), the outer growth rate (Eq. (8)) and the bulk concentration (Eq. (10)). This system of ODEs is solved by Runge-Kutta method of 4th order. As initial conditions, the bulk is considered saturated and the inner and outer radius are considered equal to the droplet radius. The water permeation rate, Eq. (6), is evaluated explicitly and has initial value of zero. All particles are considered to be equal and agglomeration is neglected; thence, the sum term of Eq. (10) becomes a multiplication by the number of particles i in the system.

Results and Discussions

The model is compared with experimental results from Melchuna et al. [13] for gas consumption due to hydrate formation in a flowloop of 40 m length and 10.2 mm ID. The fluids considered are methane, deionized water and Kerdane (a light oil with C11 to C14 composition). The case of 40% water cut and 1.36 m/s of mixture superficial velocity was chosen for comparison with the model (water-in-oil emulsion flow). The main characteristics of the experiment are shown in Table 1. The values of the closure parameters used for the model evaluation are presented in Table 2.

Table 1. Characteristics of the experiments of Melchuna et al. [13,14].

Fluids	Methane, deionized water, Kerdane
Water cut	40%
Pressure	80 bar
Temperature	275.5 K
Mixture superficial velocity	1.36 m/s
Total liquid volume in the flowloop	10 L

The number of particles i in the system is estimated by the use of the droplet radius and the total volume of water in the system as:

$$i = \frac{\forall_w}{\forall_{droplet}} \alpha = \frac{3}{4} \frac{WC \times \forall_{total}}{\pi r_{droplet}^3} \alpha \tag{11}$$

Factor α is introduced to represent the efficiency of particles that are consuming gas. This efficiency is related to the amount of particles that are actually in contact with the bulk, that is, an efficiency due to the impossibility of mass transfer between the particles and the bulk for a dense dispersion and for long distances from the oil-gas interface to the particle.

Figure 2 presents the evolution in time of the gas consumption due to hydrate formation. The model is capable of representing the experimental results with the order of magnitude of the closure parameters presented in literature (Table 2) and for a curve fitting of $\alpha \approx 2.4\%$. Initially, hydrates form fast since only crystal integration resistances are present. However, the gas consumption rate decreases with time, with an asymptotic trend related to increased diffusion and permeation resistance as the hydrate shell thickens.
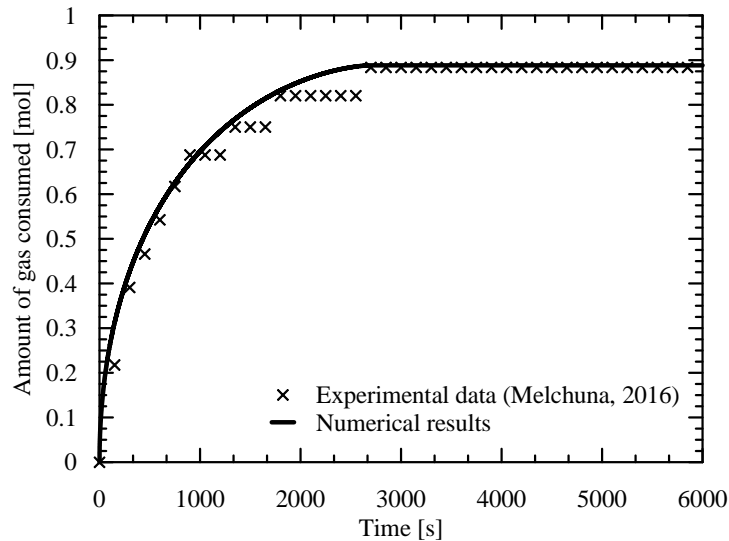

Figure 2. Comparison of model results against experimental data of Melchuna et al. [14] for the amount of gas consumed over time due to hydrate formation.

Table 2. Closure parameters used for model evaluation.

Parameter	Value adopted
Gas diffusivity in hydrate (Davies et al. 2008, apud [15])	$D_h = 4 \times 10^{-13}$ m^2/s
Solubility of gas in solids (order of magnitude from [16])	$S_h = 10^{-1} \dfrac{\text{mol gas}}{\text{mol solid}}$ (at 80 bar)
Mass transfer coefficient around a spherical particle (Armenante and Kirwan 1989, apud [11]; estimated for the range of r_{out} calculated by the model)	$h_m = (0.15 - 1.31) \times 10^{-3} \dfrac{m}{s}$
Constant of proportionality of crystal integration process (order of magnitude from [4])	$k_i \approx 6 \times 10^{-10} \dfrac{\text{mol}}{\text{m}^2\text{sPa}}$
Henry's constant of methane in water [17]	$H_w = 8.9 \times 10^{-6} \dfrac{mol}{m^3 Pa}$
Henry's constant of methane in Kerdane (calculate from solubility measurements of [14])	$H_o \approx 2.4 \times 10^{-4} \; mol / (m^3 Pa)$
Absorption coefficient (experimental results of [14] for the analyzed case of Table 1)	$\dfrac{k_{g/o} A_{g/o}}{\forall_o} \approx 8.1 \times 10^{-3} s^{-1}$
Properties of methane sI hydrates [15] Assumption: hydrate kinetics cause less cage occupancy	$\rho_h \approx 917 \, kg/m^3 \; ; \; M_h \approx 17.7 \, g/mol$ $\eta = 6$
Kerdane properties [18] Assumption: diffusivity of methane in Kerdane is one order of magnitude higher than methane in water.	$\rho_o \approx 815 \, kg/m^3 \; ; \; \mu_o \approx 3 \times 10^{-3} \, Pa.s$ $D_{g/o} = 1.5 \times 10^{-9} \dfrac{m^2}{s}$
Equilibrium pressure for the given temperature (CSMGem, [19])	$P_{eq} = 32.5 \times 10^5 \, Pa$
Equilibrium fugacity (ideal gas)	$f_{eq} = P_{eq}$
Gas fugacity at gas free phase (ideal gas)	$f_g = P = 80 \times 10^5 \, Pa$
Droplet size (experimental measurements of [14] for the analyzed case of Table 1)	$r_{droplet} = 23 \mu m$

Conclusions

This study extended the predictive models for hydrate growth in gas-oil-water systems presented by literature. The model was compared with experimental data and the trend of gas consumption over time was validated. The model captures the fast initial growth rate of the hydrates, with an asymptotic trend as the hydrate shell imposes higher mass transfer resistances. The mass transfer resistances are associated with gas diffusion and water permeation trough the hydrate shell, which are related to the shell width and therefore increase in time as the shell becomes thicker.

Nomenclature

C Gas concentration [mol/m^3]
D_h Mass diffusivity of gas inside hydrates [m^2/s]
H_w Henry's constant of gas inside water [mol/(m^{3}Pa)]
h_m Mass transfer coefficient [m/s]
i Number of hydrate particles in the system [-]
k_i Constant of proportionality of the crystal integration rate [mol/(m^2.s.Pa)]
$k_{g/o}$ Absorption coefficient of gas by oil [m/s]
$-dn_g/dt\big|_{hyd}$ Gas consumption rate due to hydrate formation [mol/s]

Q Water permeation flowrate through the hydrate shell [m^3/s]
r_{in}, r_{out} Inner and outer radius of the hydrate particle [m]
$\forall$ Volume [m^3]
WC Water cut [-]
η Hydration number [-]

Indexes
b Bulk
eq Three-phase gas-water-hydrate equilibrium

g	Gas		o	Oil
h	Hydrates		out	Outer surface of the particle
i	Referent to one particle		w	Water
in	Inner surface of the particle			

Acknowledgements

References

[1]   E.D. Sloan, C.A. Koh (2008): **Clathrate hydrates of natural gases**, 3rd ed., *Taylor & Francis Group*, Boca Raton, USA.

[2]   D. Sloan, C. Koh, A.K. Sum (2011): **Natural gas hydrates in flow assurance**, 1st ed., Elsevier Inc., Burlington, USA.

[3]   D.J. Turner, K.T. Miller, and E.D. Sloan (2009): **Methane hydrate formation and an inward growing shell model in water-in-oil dispersions**, *Chem. Eng. Sci.* 64, 3996–4004.

[4]   B.H. Shi, J. Gong, C.Y. Sun, J.K. Zhao, Y. Ding, and G.J. Chen (2011): **An inward and outward natural gas hydrates growth shell model considering intrinsic kinetics, mass and heat transfer**, *Chem. Eng. J.* 171, 1308–1316.

[5]   C.L. Bassani, F.A.A. Barbuto, A.K. Sum, R.E.M. Morales (2018): **A three-phase solid-liquid-gas slug flow mechanistic model coupling hydrate dispersion formation with heat and mass transfer**, *Chem. Eng. Sci.* 178, 222–237.

[6]   C.L. Bassani, F.A.A. Barbuto, A.K. Sum, R.E.M. Morales (2017): **Hydrate formation effects on slug flow hydrodynamics and heat transfer: wall deposition vs. dispersion formation**, in: *IV Journeys Multiph. Flows*, JEM-2017-0015, São Paulo, Brazil.

[7]   S. Peker, S. Helvaci (2007): **Solid-liquid two-phase flow**, 1st ed., *Elsevier Science*, Amsterdam, Netherlands.

[8]   C.P. Ribeiro Jr, P.L.C. Lage (2008): **Modelling of hydrate formation kinetics: State-of-the-art and future directions**, *Chem. Eng. Sci.* 63, 2007–2034.

[9]   Z. Yin, Z.R. Chong, H.K. Tan, P. Linga (2016): **Review of gas hydrate dissociation kinetic models for energy recovery**, *J. Nat. Gas Sci. Eng.* 35, 1362–1387.

[10]   P. Englezos, N. Kalogerakis, P.D.D. Dholabhai, P.R.R. Bishnoi (1987): **Kinetics of formation of methane and ethane gas hydrates**, *Chem. Eng. Sci.* 42, 2647–2658.

[11]   J.M. Herri, J.S. Pic, F. Gruy, M. Cournil (1999): **Methane hydrate crystallization mechanism from in-situ particle sizing**, *AIChE J.* 45, 590–602.

[12]   N. Brauner (2001): **The prediction of dispersed flows boundaries in liquid-liquid and gas-liquid systems**, *Int. J. Multiph. Flow.* 27, 885–910.

[13]   A. Melchuna, A. Cameirao, J.M. Herri, P. Glenat (2016): **Topological modeling of methane hydrate crystallization from low to high water cut emulsion systems**, *Fluid Phase Equilib.* 413, 158–169.

[14]   A.M. Melchuna (2016): **Experimental study and modeling of methane hydrates crystallization under flow from emulsions with variable fraction of water and anti-agglomerant**, PhD Thesis, Mines Saint Etienne, Saint Etienne, France.

[15]   J.W. Jung, D.N. Espinoza, J.C. Santamarina (2010): **Properties and phenomena relevant to CH4-CO2 replacement in hydrate-bearing sediments**, *J. Geophys. Res. Solid Earth.* 115, B10102.

[16]   R.M. Barrer (1941): **Diffusion in and through solids**, 1st ed., *The Cambridge Series of Physical Chemistry*, Cambridge, UK.

[17]   R. Sander (1999): *Compilation of Henry's law constants for inorganic and organic species of potential importance in environmental chemistry*, Mainz, Germany.

[18]   Total (2015): **Kerdane D 75 Safety Data Sheet**.

[19]   A.L. Ballard, E.D. Sloan (2004): **The next generation of hydrate prediction IV: A comparison of available hydrate prediction programs**, *Fluid Phase Equilib.* 216, 257–270.